ISSN 2075-1133, Inorganic Materials: Applied Research, 2015, Vol. 6, No. 5, pp. 466–472. © Pleiades Publishing, Ltd., 2015.
Original Russian Text © A.B. Sivak, P.A. Sivak, V.A. Romanov, V.M. Chernov, 2015, published in Perspektivnye Materialy, 2015, No. 1, pp. 31–40.

Effect of External Stresses on Efficiency of Dislocation Sinks in BCC (Fe, V) and FCC (Cu) Crystals

A. B. Sivak[a, b], P. A. Sivak[a], V. A. Romanov[b, c], and V. M. Chernov[b, d]

[a] *National Research Centre "Kurchatov Institute", Moscow, 123182 Russia*
[b] *National Research Tomsk State University, Tomsk, 634050 Russia*
[c] *State Scientific Centre of the Russian Federation – Institute for Physics and Power Engineering, Obninsk, 249033, Russia*
[d] *A.A. Bochvar High-technology Research Institute of Inorganic Materials (VNIINM), Moscow, 123098 Russia*
e-mail: sivak_ab@nrcki.ru, sivak_pa@nrcki.ru, romanov-ippe@mail.ru, chernov@bochvar.ru

Received June 2, 2014

Abstract—The efficiency of linear sinks for self-point defects (SPDs) elastically interacting (dislocations) and not interacting with sinks with the density of 3×10^{14} m^{-2} is calculated for BCC (Fe, V) and FCC (Cu) crystals at the temperature 293 K using the object kinetic Monte Carlo technique, depending on type and value of applied mechanical load (up to 200 MPa) and types of linear sinks. Full straight dislocations in slip systems $[111](1\bar{1}0)$, $[111](11\bar{2})$, [100](001), and [100](011) for Fe and V and [100](001) for Cu are considered for dislocation sinks (DSs). Orientations of noninteracting linear sinks (NILSs) coincide with those of DSs. Interaction of SPDs with internal (dislocation) and external stress fields is calculated within the framework of anisotropic linear theory of elasticity. Relative changes in efficiency of different co-directional linear sinks (either interacting or not interacting with SPDs) under action of applied stress are approximately identical under low stress. Radiation creep rates are calculated for the considered crystals under uniaxial stress in the stationary regime of Frenkel pairs generation. The creep rate strongly depends on the loading direction and Burgers vector of dislocations in Fe and V, and it is almost independent of these parameters in Cu. At the same generation rate of Frenkel pairs, the radiation creep rate averaged over all loading directions is significantly higher in BCC (Fe, V) crystals containing dislocations with the Burgers vector $a/2\langle 111\rangle$ than in FCC (Cu) crystals.

Keywords: efficiency of dislocation sinks, self-point defects, diffusion, external stresses, object kinetic Monte Carlo
DOI: 10.1134/S2075113315050184

INTRODUCTION

In [1], different mechanisms of crystal deformation caused by radiation impact under stress were considered, and it was shown that the strongest effect has stress-induced diffusion anisotropy of radiation point defects. This diffusion anisotropy of defects causes a dependence of efficiency of dislocation sinks (DSs) for radiation defects on applied external loads, which results in redistribution of the balance of flows of self-interstitial atoms (SIAs) and vacancies to dislocations differently oriented with respect to external load and in a consequent dislocation climb. In order to estimate the radiation-induced deformation rate of a crystal under given external load determined by climb of edge dislocations, it is necessary to know the dependence of efficiency of DSs of radiation defects on applied external loads within the framework of anisotropic diffusion of self-point defects (SPDs), which was not done in [1].

When calculating the dependences, it is necessary to use methods and approaches sensitive to real crystal symmetry, since these mechanisms of radiation-induced deformation of a crystal are determined by anisotropic effects. An analytical solution for efficiency of DSs interacting with SPDs is absent, and numerical simulation should be used for its finding.

The purpose of the present work is to establish the dependence of DSs on applied external loads for anisotropic BCC (Fe, V) and FCC (Cu) crystals using the object kinetic Monte Carlo method [2, 3].

The efficiency of linear sinks for diffusing SPDs not interacting with the sinks and absorbed, if captured, by a sink core with a certain absorption radius (NILSs, noninteracting linear sinks) will be calculated for comparison. Directions, densities, and absorption radii of NILSs correspond to DSs interacting with SPDs.

Interaction of SPDs, considered as elastic dipoles, with dislocations and external stress fields is calculated within the framework of anisotropic linear theory of elasticity [4, 5]. In this case, the crystallographic (right) coordinate system was used; indices "+" or "–"

were added to a name of a value designating its association with an SIA or a vacancy, respectively.

COMPUTER MODEL

Self-Point Defects

The characteristics of SPDs (formation energy and dipole tensor of the SPDs for stable and saddle-point configurations) for BCC (Fe, V) and FCC (Cu) crystals used for the calculations in this work were obtained in [7, 8] using molecular statics simulation. Though molecular dynamics modeling [9, 10] with the use of the same potentials of interatomic interaction as in [7, 8] has shown that diffusion of SIAs and vacancies can proceed via different mechanisms, in this work in modeling of SPDs with the object kinetic Monte Carlo method, only basic diffusion mechanisms were taken into account:

—in the case of SIAs, a jump of ⟨110⟩ dumbbell to the nearest site with rotation of the dumbbell axis by 60° for BCC (Fe, V) crystals and a jump of ⟨100⟩ dumbbell to the nearest site with rotation of the dumbbell by 90° for FCC (Cu) crystal;

—for vacancies, a jump of atom from a lattice site to the nearest vacant site.

DSs and NILSs

For BCC crystals, straight full edge and screw dislocations, EDs and SDs, with Burgers vectors $a/2[111]$ and $a[100]$ (where a is the lattice parameter) are considered in the slip systems $[111](1\bar{1}0)$, $[111](11\bar{2})$, $[100](001)$, and $[100](011)$.

For the FCC Cu crystal, a straight full ED with Burgers vector $a/2[110]$ is considered in the slip system $[110](001)$.

Also, NILSs lying in the crystallographic directions ⟨100⟩, ⟨110⟩, ⟨111⟩, and ⟨112⟩ are considered for BCC and FCC crystals.

External Loading

Six different types of loading are used for calculation of efficiency of SPD sinks: one of six independent components of the external stress tensor assumes the value σ; the other five are zero. For convenience hereinafter, the respective type of loading will be designated as a nonzero component of a stress tensor, for example, σ_{12}. For FCC crystals, all six types of loading were calculated, and for BCC, only three, σ_{12}, σ_{13}, and σ_{23}, since diagonal components of the stress tensor do not cause anisotropy of SPD diffusion and, therefore, have no impact on efficiency of the sinks in BCC crystals because of special features of symmetry of the BCC lattice (loading axes σ_{11}, σ_{22}, and σ_{33} lie along the 4-fold symmetry axis) and diffusion mechanisms (SPD jump is along the 3-fold symmetry axis). The calculations were performed for σ values of ±40, ±80, ±120, ±160, and ±200 MPa.

Interaction of SPDs with Sinks and External Stress Fields

Interaction energy of SPDs in stable and saddle-point configurations with dislocations and external stress fields was calculated within the framework of anisotropic theory of elasticity [4, 5, 11]:

$$E^{\text{int}} = -P_{ij}S_{ijkl}(\sigma^{d}_{kl} + \sigma_{kl}), \quad (1)$$

where P_{ij} is the dipole tensor of SPDs, S_{ijkl} is the elastic compliance tensor, σ^{d}_{kl} and σ_{kl} are the tensors of dislocation and external stress fields, and summation is performed over repeated indices ($i, j, k, l = 1, 2, 3$). The same values of elastic constants (c_{11}, c_{12}, c_{14}) and the lattice parameter were used as in [7, 8].

Comparison of the results of calculation of interaction energy between SPDs and dislocation and external stress fields using molecular statics and anisotropic theory of elasticity has shown their good agreement [9, 12].

Sinks Efficiency

Calculation of sinks efficiency $\xi = k^2/\rho_d$, where k^2 is the sink strength (k^{-1} is diffusion length before absorption at a sink) and ρ_d is the density of DSs or NILSs, was performed by object kinetic Monte Carlo method following [8, 9, 13].

In a model crystal, there is only one SPD and one type of sink (in this work, either DS or NILS of a definite type). The starting positions of SPDs were randomly given in a crystallite. The model crystal is a right-angle prism of infinite length, which has a square with the side length L as a base. The DS or NILS was in the center of the prism. Periodic boundary conditions were imposed on the lateral faces of the prism: in the case where the SPD left the crystallite, it was returned from the opposite face of the crystallite. Thus, a crystal for modeling contained square net of parallel linear sinks spaced at a distance L, which corresponds to the density of sinks L^{-2}. The value L was chosen to be $200a$ and $160a$ for BCC and FCC crystals, respectively. Therefore, the density of sinks is $\sim 3 \times 10^{14}$ m^{-2}, which corresponds to a typical value of dislocation density in deformed and irradiated metals. The trajectory of an SPD was calculated until a defect was absorbed by a sink (approaching to a distance smaller than r_0 to a sink). After that, an SPD of the same type was inserted into the model crystal. The sink efficiency ξ is expressed by the relation [8, 9, 13]

$$\xi = \frac{2dL^2}{l^2\langle N\rangle}, \quad (2)$$

Efficiency of NILSs in the absence of external loads, $\xi_0^{\pm}(0)$ ("+" for SIAs, "–" for vacancies), in BCC and FCC crystals with density of linear sinks of $(200a)^{-2}$ and $(160a)^{-2}$, respectively. Relative error is less than 0.05%

Noninteracting linear sink	Efficiency of NILSs in crystals			
	BCC		FCC	
	$\xi_0^+(0)$	$\xi_0^-(0)$	$\xi_0^+(0)$	$\xi_0^-(0)$
NILS ⟨100⟩	2.104	2.107	2.104	2.106
NILS ⟨110⟩	2.101	2.106	2.098	2.100
NILS ⟨111⟩	2.094	2.098	2.106	2.107
NILS ⟨112⟩	2.100	2.106	2.104	2.105

where l is the length of a jump equal to $a\,3^{1/2}$ and $a\,2^{1/2}$ in BCC and FCC lattices, respectively; $\langle N\rangle$ is the average number of jumps of an SPD before absorption at a sink; and $d = 3$ is the dimensionality of motion.

For BCC crystals, r_0 is chosen to be $2.4a$, in order to reach geometrical similarity of the model for BCC and FCC crystals, i.e., so that the ratio L/r_0 would not depend on choice of material. Some ambiguity in the criterion of choice of the r_0 value does not have a considerable effect on the calculated values of DS efficiencies, since field interaction between SPDs and dislocations makes the determining contribution to the ξ value [14].

The effect of splitting of a full dislocation into two partial Shockley dislocations on DS efficiency in Cu was not taken into account [13].

Accuracy of the Calculations

To obtain statistically reliable data on the effect of loading on sink efficiency, such a number of trajectories was calculated as to make the statistical error of the result no more than 0.3% (the confidence probability was taken as 99%). This accuracy was provided by modeling over 10^6 SPD trajectories. Since relative changes in efficiency of DSs and NILSs under loading were compared, estimates of efficiencies of the sinks without loading were even more exact: 0.1% and 0.05% for DSs and NILSs, respectively. In some cases, symmetry of the considered problem led to the same change in efficiency of a sink under action of different applied loading types. In these cases, the accuracy of the calculations increased additionally.

RESULTS

Sink Efficiencies without Applied External Loads

The DSs efficiencies in BCC and FCC crystals calculated by the object kinetic Monte Carlo method in the absence of external loads are presented in [8, 9, 13, 14]. In the case of NILSs, the results (table) are determined only by symmetry of a crystal (for the considered diffusion mechanisms of SPDs), since the interaction energy between an SPD and a sink, which determines the specifics of a particular material, is zero. Therefore, in table, the results are separated only by symmetry of a crystal without mentioning a particular material.

The Effect of Applied Loads on Sink Efficiencies

The effect of external loading on the efficiency of DSs and NILSs in BCC (Fe, V) and FCC (Cu) crystals was calculated for all types of sinks and external stresses considered in the work. Since the results are numerous, Fig. 1 shows typical examples of the efficiency of sinks for the considered crystals. For the approximations used (frequencies of SPD jumps are determined by Arrhenius type dependences, and it is assumed that the pre-exponential factor does not depend on external stress field [8, 9, 13]), the NILSs efficiency depends only on the ratio between the load σ and absolute temperature T; therefore, an additional x axis is added in Fig. 1 for the σ/T parameter.

Also, the results of calculations of the NILSs efficiencies obtained with Saralidze's analytic solution [1, 6] are shown for comparison:

$$\frac{\xi_0(\sigma_{ij})}{\xi_0(0)} = \frac{3D_\perp}{\mathrm{Tr}D_{ij}}, \qquad (3)$$

where $\xi_0(\sigma_{ij})$ is the NILSs efficiency under applied external stress field, $\xi_0(0)$ is the NILSs efficiency in the absence of external stress field, $\mathrm{Tr}D_{ij}$ is the trace of the SPD diffusion tensor, and $D_\perp$ is the average diffusion coefficient in the plane normal to NILS orientation.

Figure 1 considers types of loading at which only one component of the external stresses tensor σ_{ij} is nonzero. For the sinks considered in Figs. 1a and 1b, the loading types σ_{12} and σ_{23} are crystallographic equivalents; in Figs. 1c and 1d, the crystallographic equivalents are σ_{13} and σ_{23}; in Figs. 1e and 1f, they are σ_{11} and σ_{22} and also σ_{13} and σ_{23}.

In the linear approach for the aforementioned diffusion mechanisms of SIA (+) and vacancy (–) in BCC crystals, the effect of external stresses on the

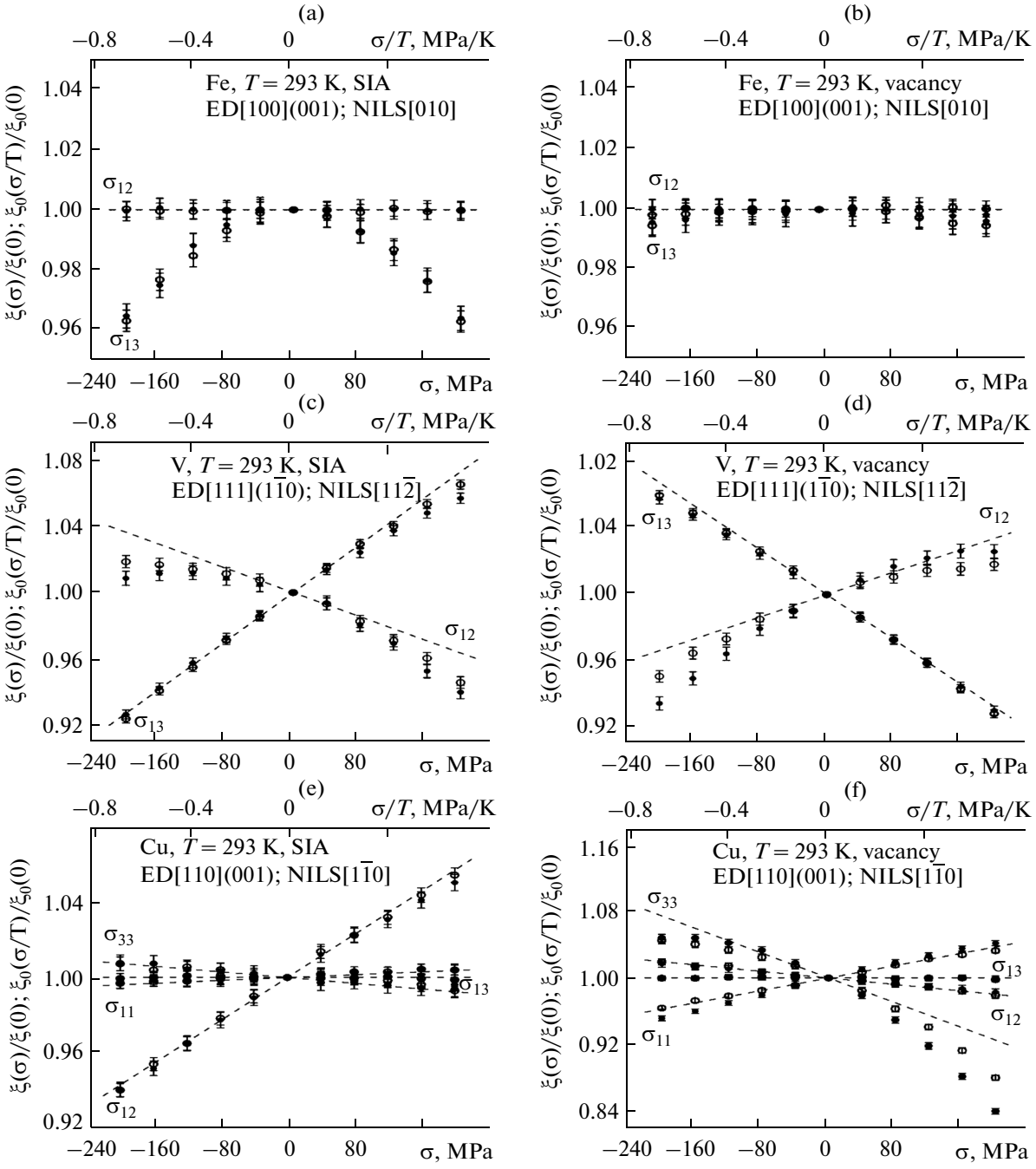

Fig. 1. Dependences of efficiencies of DSs and NILSs on applied load σ for SIA (a, c, e) and vacancy (b, d, f): (a, b) ED[100](001) and NILS [100], respectively, in BCC Fe crystal; (c, d) ED[111](1$\bar{1}$0) and NILS [11$\bar{2}$], respectively, in BCC V crystal; (e, f) ED[110](001) and NILS[1$\bar{1}$0], respectively, in FCC Cu crystal at 293 K. Solid and open symbols are for DSs and NILSs, respectively. Dashed lines are Saralidze's solution [1, 6].

form of the $D_{ij}^{\pm}$ tensor can be written as (no summing over repeated indices):

$$\frac{3D_{ij}^{\pm}}{\mathrm{Tr}D_{ij}^{\pm}} = \delta_{ij} + \frac{P^{\pm}\beta}{c_{44}}\sigma_{ij}(1-\delta_{ij}), \qquad (4)$$

where δ_{ij} is the Kronecker symbol, $P^{-} = P_{12}^{-}$, $P^{+} = (P_{12}^{+} + P_{13}^{+} + P_{23}^{+})/3$, $P_{ij}^{\pm}$ is the dipole tensor of SPD in a saddle-point configuration responding to a jump in the [111] direction, $\beta = (k_B T)^{-1}$, and k_B is the Boltzmann constant.

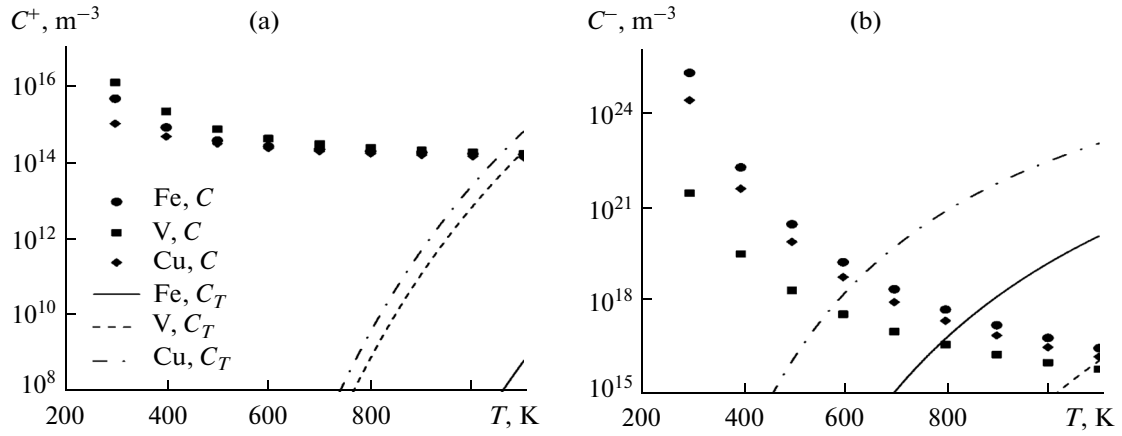

Fig. 2. Temperature dependence of stationary concentrations of thermal C_T and radiation C: (a) SIAs, (b) vacancies in Fe, V, and Cu at the Frenkel pair formation rate (per atom) 10^{-7} s^{-1} and dislocation density 3×10^{14} m^{-2}.

For FCC crystals, the similar relationship is (no summing over repeated indices)

$$\frac{3D_{ij}^{\pm}}{\mathrm{Tr}D_{ij}^{\pm}} = \delta_{ij} + \frac{P_n^{\pm}\beta}{c_{44}}\sigma_{ij}(1-\delta_{ij}) + \frac{P_d^{\pm}\beta}{c_{11}-c_{12}}\left(\sigma_{ij} - \frac{\mathrm{Tr}\sigma_{ij}}{3}\right)\delta_{ij}, \quad (5)$$

where $P_n^{\pm} = P_{12}^{\pm}/2$, $P_d^{+} = 9(P_{11}^{+} - P_{33}^{+})/16$, $P_d^{-} = (P_{11}^{-} - P_{33}^{-})/2$, and $P_{ij}^{\pm}$ is the dipole tensor of SPD in the saddle-point configuration corresponding to jump in [110] direction.

Saralidze's solution [1, 6] describes NILSs efficiency with accuracy no worse than 1% at $|\sigma/T| \le 0.34$ MPa/K (here, σ is the maximum component of the stress tensor) for all types of loadings and NILSs in the considered Fe, V, and Cu crystals.

Comparison of the object kinetic Monte Carlo data for efficiencies of DSs and co-directional NILSs leads to a conclusion that their relative changes under load are approximately coincident:

$$\frac{\xi(\sigma_{ij})}{\xi(0)} \approx \frac{\xi_0(\sigma_{ij})}{\xi_0(0)}. \quad (6)$$

Therefore, to describe changes in DS efficiencies, it is also possible to use Saralidze's solution. The range of its validity is narrower than for NILSs: accuracy no worse than 1% at $|\sigma/T| \le 0.27$ MPa/K at $T = 293$ K. As the temperature increases, the range of validity of Saralidze's solution for DSs determined by the $|\sigma/T|$ ratio tends to the range of validity of Saralidze's solution for NILSs. Thus, at $T = 1000$ K, Saralidze's solution can be applied for DSs at $|\sigma| < \sim 300$ MPa, which covers the working range of external loadings for structural materials of the cores of nuclear fission and fusion reactors.

The DSs efficiency in BCC crystals does not depend on diagonal elements of the external stress tensor, owing to specifics of the lattice symmetry and diffusion mechanisms of SPDs.

DISCUSSION

The obtained dependences of DSs efficiency on external loading values make it possible to calculate the radiation creep rate governed by climbing of edge dislocations.

We shall consider a case where radiation provides stationary concentrations of SIAs and vacancies which surpass considerably the equilibrium concentrations. Figure 2 shows the calculated temperature dependences of stationary concentrations of radiation and thermal SPDs.

The stationary concentrations of radiation SPDs were calculated neglecting recombination as follows:

$$C = \frac{G}{D\Omega\xi\rho_d}, \quad (7)$$

where $G = 10^{-7}$ s^{-1} is the Frenkel pair generation rate (number of Frenkel pairs per atom per second), Ω is the atomic volume, $\rho_d = 3 \times 10^{14}$ m^{-2}, D are the diffusion coefficients of SPDs (the values are taken from [9, 10, and 15] for Fe, V, and Cu, respectively), and ξ is DSs efficiency (ED $\langle 111\rangle\{110\}$ for Fe and V, ED $\langle 110\rangle\{001\}$ for Cu). At the mentioned values of the parameters, the consideration for recombination results in changes in C values within 5% from the values calculated by Eq. (7) at $T \ge 400$ K.

The thermal concentration of SPDs was derived from the formula

$$C_T = \exp(-E^F\beta), \quad (8)$$

where E^F is the formation energy of SPDs. The contribution from the formation entropy of SPDs to the thermal concentration (additional entropy factor $\exp(S^F/k_B)$ in the right part of Eq. (8)) was not taken

into account. The value S^F/k_B for vacancies, according to different estimates, is mainly in the range from 0 to 4 [15–17]; for SIAs, the spread is wider: from –2 to 10 [15, 17–19]; i.e., real values of thermal concentrations can differ from those presented in the figure by two orders of magnitude for vacancies and by four orders of magnitude for SIAs.

It is seen from Fig. 2 that, for the considered conditions, the relation $C_T \ll C$ is satisfied for SIAs up to 1000 K for Fe, V, and Cu; for vacancies, it is satisfied up to 600, 800, and 1000 K for Cu, Fe, and V, respectively.

The deformation rate of a crystal in the Burgers vector direction of climbing dislocations of the family i is [1]

$$\dot{\varepsilon}_i = \rho_{d,i} b_i v_i = \Omega \rho_{d,i} (I_i^+ - I_i^-), \quad (9)$$

where v_i is the climbing rate of dislocations i and $I_i^\pm$ are the SPD flows per unit length of dislocation i:

$$I_i^\pm = \xi_i^\pm D^\pm C^\pm. \quad (10)$$

If the recombination is small,

$$D^\pm C^\pm = G\left(\Omega \sum_{i=1}^{n} \xi_i^\pm \rho_{d,i}\right)^{-1}, \quad (11)$$

where n is the number of dislocation families.

If there is no texture in a crystal ($\rho_{d,1} = \rho_{d,2} = ... = \rho_{d,n} = \rho_d/n$), substitution of (10) and (11) into (9) gives an expression for the contribution from the dislocation family i to the deformation rate:

$$\dot{\varepsilon}_i = \frac{G}{n}\left(\frac{\xi_i^+(\sigma)}{\xi_i^+(0)} - \frac{\xi_i^-(\sigma)}{\xi_i^-(0)}\right). \quad (12)$$

BCC Fe and V Crystals

In the case where there are only dislocations with $b = a/2\langle 111\rangle$ in a crystal, use of (3)–(6) and (12) gives the following expressions for deformation rates in the uniaxial loading directions ⟨111⟩, ⟨110⟩, and ⟨100⟩:

$$\dot{\varepsilon}_{\langle 111\rangle} = \frac{G\beta\sigma}{27}\frac{P^+ - P^-}{c_{44}},$$

$$\dot{\varepsilon}_{\langle 110\rangle} = \frac{G\beta\sigma}{36}\frac{P^+ - P^-}{c_{44}},$$

$$\dot{\varepsilon}_{\langle 100\rangle} = 0.$$

At uniaxial loading of 100 MPa in the ⟨111⟩ direction and $T = 600$ K, the creep rate in the loading direction is $3.6 \times 10^{-3}\ G$ and $3.8 \times 10^{-3}\ G$ for Fe and V, respectively.

If there are only dislocations with $\mathbf{b} = a\langle 100\rangle$, the radiation creep rate is zero for any type of loading.

FCC Cu Crystal

In the case where a crystal contains only dislocations with $\mathbf{b} = a/2\langle 110\rangle$, use of (3)–(6) and (12) gives for the deformation rates in the uniaxial directions ⟨111⟩, ⟨110⟩, and ⟨100⟩ the following expressions:

$$\dot{\varepsilon}_{\langle 111\rangle} = \frac{G\beta\sigma}{36}\frac{P_n^+ - P_n^-}{c_{44}},$$

$$\dot{\varepsilon}_{\langle 110\rangle} = \frac{G\beta\sigma}{48}\left(\frac{P_n^+ - P_n^-}{c_{44}} + \frac{P_d^+ - P_d^-}{6(c_{11} - c_{12})}\right),$$

$$\dot{\varepsilon}_{\langle 100\rangle} = \frac{G\beta\sigma}{72}\frac{P_d^+ - P_d^-}{c_{11} - c_{12}}.$$

Under uniaxial load of 100 MPa in the ⟨111⟩ and ⟨100⟩ directions at $T = 600$ K, the creep rate in the loading direction is $1.1 \times 10^{-3}\ G$ and $1.4 \times 10^{-3}\ G$, respectively: the creep rate depends only slightly on loading direction in a FCC Cu crystal.

On average, in all loading directions, the creep rate is lower by a factor of two in FCC Cu crystal containing dislocations with $\mathbf{b} = a/2\langle 110\rangle$ than in BCC Fe and V crystals containing dislocations with $\mathbf{b} = a/2\langle 111\rangle$ at the same Frenkel pair generation rate.

CONCLUSIONS

1. The efficiencies of linear sinks for radiation point defects interacting (dislocations) or not interacting with such sinks at the temperature of 293 K in BCC (Fe and V) and FCC (Cu) crystals with the sink density of $\sim 3 \times 10^{14}$ m^{-2} under action of external loading of different types and values (up to 200 MPa) were calculated by the object kinetic Monte Carlo method. The energies of interaction between SPDs and external or dislocation stress fields were calculated within the framework of anisotropic linear theory of elasticity.

2. The relative changes in efficiencies of dislocation and noninteracting linear sinks under applied load coincide at relatively small loads, which substantiates using analytical solution (3) for NILS, accurately describing the obtained data as functions of temperatures and loads in the calculated ranges, for description of the effect of external loading on efficiency of dislocation sinks.

3. BCC symmetry of a crystal lattice results in specifics of the obtained dependences of sinks efficiency on applied loads:

—Dislocations sinks efficiency does not depend on diagonal elements of tensors of external stresses.

—Dislocations sinks efficiency depends slightly on any type of external loads if dislocations lie in ⟨100⟩ directions.

4. Radiation creep rates for the considered BCC and FCC crystals owing to edge dislocation climb (of dislocations uniformly distributed in all slip systems) are obtained at a stationary rate of Frenkel pair formation for some particular cases, and it is shown that

—in a crystal class, numerical results for radiation creep rate differ insignificantly for different BCC materials (Fe and V);

—in the BCC crystal containing only dislocations with $\mathbf{b} = a\langle 100\rangle$, the creep rate is zero at any type of external loads;

—the creep rate depends strongly on uniaxial loading direction in BCC (Fe, V) (for example, it is zero under uniaxial load in the $\langle 100\rangle$ direction) and is almost independent of it in FCC Cu crystal;

—the creep rate averaged over all directions in FCC Cu crystal containing dislocations with $\mathbf{b} = a/2\langle 110\rangle$ is half that in BCC crystals (Fe and V) containing dislocations with $\mathbf{b} = a/2\langle 111\rangle$.

REFERENCES

1. Saralidze, Z.K. and Indenbom, V.L., Dislocations in irradiated crystals, in *Elastic Strain Fields and Dislocation Mobility*, Indenbom, V.L. and Lothe, J., Eds., Amsterdam: Elsevier, 1992.
2. Domain, C., Becquart, C.S., and Malerba, L., Simulation of radiation damage in Fe alloys: An object kinetic Monte Carlo approach, *J. Nucl. Mater.*, 2004, vol. 335, pp. 121–145.
3. Caturla, M.J., Diaz de la Rubia, T., and Fluss, M., Modeling microstructure evolution of f.c.c. metals under irradiation in the presence of He, *J. Nucl. Mater*, 2003, vol. 323, pp. 163–168.
4. Hirth, J.P. and Lothe, J., *Theory of Dislocations*, New York: Wiley, 1982.
5. Kröner, E., Allgemeine Kontinuumstheorie der Versetzungen und Eigenspannungen, *Arch. Rational Mech. Anal.*, 1959–1960, vol. 4, pp. 273–334.
6. Saralidze, Z.K., Radiational growth due to diffusional anisotropy, *Sov. At. Ener.*, 1978, vol. 45, pp. 697–700.
7. Sivak, A.B., Chernov, V.M., Dubasova, N.A., and Romanov, V.A., Anisotropy migration of self-point defects in dislocation stress fields in BCC Fe and FCC Cu, *J. Nucl. Mater.*, 2007, vol. 367–370, pp. 316–321.
8. Sivak, A.B., Chernov, V.M., Romanov, V.A., and Sivak, P.A., Kinetic Monte-Carlo simulation of self-point defect diffusion in dislocation elastic fields in bcc iron and vanadium, *J. Nucl. Mater.*, 2011, vol. 417, pp. 1067–1070.
9. Sivak, A.B., Chernov, V.M., and Romanov, V.A., Diffusion of self-point defects in body-centered cubic iron crystal containing dislocations, *Crystallogr. Rep.*, 2010, vol. 55, pp. 97–108.
10. Romanov, V.A., Sivak, A.B., Sivak, P.A., and Chernov, V.M., Equilibrium and diffusion characteristics of self-point defects in vanadium, *Vopr. At. Nauki Tekhn. Ser. Termoyad. Sintez*, 2012, vol. 35, no. 2, pp. 60–80.
11. Indenbom, V.L. and Chernov, V.M., Thermally activated glide of a dislocation in a point defect field, in *Elastic Strain Fields and Dislocation Mobility*, Indenbom, V.L. and Lothe, J., Eds., Amsterdam: Elsevier, 1992.
12. Sivak, A.B., Romanov, V.A., and Chernov, V.M., Calculation of interaction of self-point defects with external stress fields in iron crystal by computer simulation and elasticity theory, *Vopr. At. Nauki Tekhn. Ser. Materialov. Nov. Mater.*, 2006, vol. 1(66), pp. 246–258.
13. Sivak, A.B. and Sivak, P.A., Efficiency of dislocations as sinks of radiation defects in fcc copper crystal, *Crystallogr. Rep.*, 2014, vol. 59, pp. 407–414.
14. Sivak, A.B., Sivak, P.A., Romanov, V.A., and Chernov, V.M., Dislocation sinks efficiency for self-point defects in iron and vanadium crystals, *Inorg. Mater. Appl. Res.*, 2015, vol. 6, pp. 105–113.
15. Suzuki, A. and Mishin, Y., Atomistic modeling of point defects and diffusion in copper grain boundaries, *Interface Sci.*, 2003, vol. 11, pp. 131–148.
16. Wolfer, W.G., Fundamental properties of defects in metals, in *Comprehensive Nuclear Materials*, Konings, R.J.M., Ed., Amsterdam: Elsevier, 2012, Vol. 1.
17. Lucas, G. and Schaublin, R., Vibrational contributions to the stability of point defects in bcc iron: A first-principles study, *Nucl. Instrum. Methods B*, 2009, vol. 267, pp. 3009–3012.
18. Ram, P.N., Green's-function calculation of entropy of formation of self-interstitials in Cu, *Phys. Rev. B*, 1984, vol. 30, pp. 6146–6153.
19. Malerba, L., Marinica, M.C., Anento, N., Nguyen, H., Domain, C., Djurabekova, F., Olsson, P., Nordlund, K., Serra, A., Terentyev, D., Willaime, F., and Becquart, C.S., Comparison of empirical interatomic potentials for iron applied to radiation damage studies, *J. Nucl. Mater.*, 2010, vol. 406, pp. 19–38.

Translated by E. Borisenko